Design Evaluation of Kitchen in the Box Stand Mixer

Sophia Gu
Mechanical Engineering,
Tufts University

Tory Hur
Mechanical Engineering,
Tufts University

Elizabeth Choi
Mechanical Engineering,
Tufts University

INTRODUCTION

The Kitchen in the Box Stand Mixer is a best-selling compact kitchen appliance designed to perform mixing tasks such as kneading dough, mixing batter, and whisking ingredients across a range of six speeds. The mixer relies on several important subsystems to convert the motor input to the rotation of the mixing attachment. Having an overall understanding of these components and how they interact is an important factor in evaluating the mixer's performance, durability, and safety.

To investigate the mixer, our team performed a teardown and engineering analysis. This process allowed us to connect the power flow from the motor to the attachment shaft to identify the main elements responsible for this motion. Based on our examination, four machine elements were selected for analysis: gear train, motor belt transmission, bearings, and shaft-torsion spring locking mechanism.

The gear train was selected for analysis as it provides the majority of the speed reduction and torque output required for the most effective mixing. The belt drive and motor were analyzed to assess how the torque is transmitted and how tension behavior can affect motion. The bearing on the motor was selected to verify load capacity and expected life, as its function as it combines loads taken from the belt and gear train. Lastly, the shaft and torsion spring system was evaluated to verify load capacity and expected life.

GEAR TRAIN

The multi-stage gear train system is responsible for stepping down the high-speed input from the motor to the low-speed, high-torque output required for mixing. The system can be identified as a compound gear train, which consists of a belt, spur, and planetary gear mechanisms, as labeled in Figure 1.

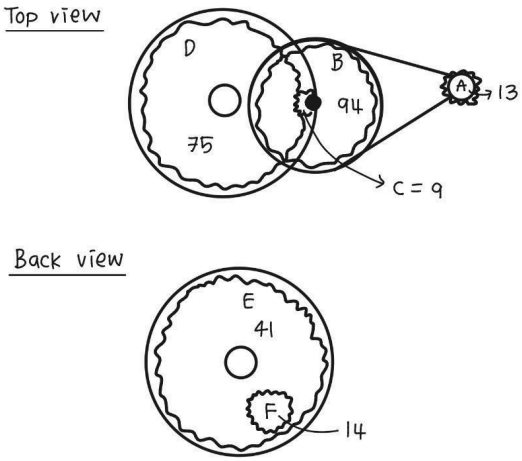


Figure 1: Schematic of the gear train system with its corresponding tooth counts.

1.1 Gear Ratio Analysis

For the stand mixer, the gear train was chosen for analysis as it consists of three distinct reduction stages, which can be analyzed by computing the gear ratio. The first stage is the belt drive, where the motor spins pinion A with 13 teeth at a high speed. This small pinion is connected by a belt train to a larger gear B with 94 teeth, providing the first significant speed reduction to a usable level for the mixer head.

$$R_{Belt} = \frac{N_B}{N_A} = \frac{94}{13} \approx 7.23 : 1$$

The second stage consists of the main gearbox, where gear B has a tiny gear hidden in the center, which is pinion C. This tiny 9-tooth gear spins against a larger gear D with 75 teeth,

which sits on the same vertical shaft. The use of a small 9-tooth pinion allows for a massive reduction ratio in a compact space.

$$R_{Gears} = \frac{N_D}{N_C} = \frac{75}{9} \approx 8.33 : 1$$

Note that for this reduction to work, Gear B and Gear C must be compound gears, where both gears spin at the same speed on the same shaft. In this stand mixer, the gears do indeed spin at the same speed on the same shaft, so we can proceed with our calculation.

The final stage occurs inside the head of the mixer that moves the beater. The central shaft that goes through gear D spins a hidden internal gear E with 41 teeth on the opposite side. The beater is attached to a planet gear F with 14 teeth that rolls along a fixed ring of gear E. By further reducing the rotational speed, this stage delivers the sustained, high-torque needed for effective mixing.

$$R_{Rings} = \frac{N_E}{N_F} = \frac{41}{14} \approx 2.93$$

Using the values obtained above, the total reduction of the gear train is

$$R_{Total} = 7.23 \times 8.33 \approx \mathbf{60.22 : 1}$$

1.2 Output Torque Analysis

Estimating the output torque is essential for validating the stand mixer's performance metric. As the stand mixer is designed to process high-viscosity materials (e.g., bread dough), quantifying this information can validate whether the theoretical gear ratios analyzed in the previous section are sufficient to generate the forces necessary for mixing without motor failure.

The transmitted power equation of

$$H = T \cdot \omega$$

where H represents power, T is the input torque, and ω is angular velocity, was used to determine the initial motor torque of the mixer. The input parameters include power (P) of 300 Watts (given value) and motor speed of roughly 13,549.5 RPM, which was calculated by

$$N_{\text{motor}} = \text{RPM} \times R_{\text{total}} = (225\,\text{RPM})(60.22) = 13{,}549.5\,\text{RPM}$$

Because manufacturer data for the operating speed of this mixer was not available, the motor speed was estimated using a comparable commercial reference. A speed of 225 rpm was selected, which corresponds to the medium speed setting on the KitchenAid Stand Mixer, which has a similar application [1]. Converting the calculated RPM into rad/s to determine the angular velocity,

$$\omega_{in} = N \times \frac{2\pi}{60} \approx \mathbf{1,419}\ \text{rad/s}$$

Given the power and angular velocity, the input torque can be calculated by deriving the above transmitted power equation,

$$T_{in} = \frac{300\ \text{W}}{1,419.6\ \text{rad/s}} \approx \mathbf{0.21}\ \text{Nm}$$

.

For calculation purposes, it was assumed that this was an ideal gear train with negligible friction due to the lubrication (grease) of the gears. In an ideal gear train, the power generated by the motor is fully transmitted to the output, therefore, energy is neither created nor destroyed. Since the two sides must be equal, if

speed reduces, the torque must go up by the same factor to keep the total power constant.

Using the speed ratio definition that torque is inversely proportional to speed, the output torque can be calculated as such:

$$\frac{T_A}{T_B} = \frac{\omega_B}{\omega_A} \quad \Rightarrow \quad T_{out} = T_{in} \times R_{total}$$

$$T_{out} = 0.21 \text{ Nm} \times 60.22 \approx \mathbf{12.65} \text{ Nm}$$

1.3 Potential Interference Conditions

Interference occurs when the tip of the driven gear digs into the root of the mating gear because the pinion has too few teeth. With only nine teeth, pinion C falls significantly below the standard limit, which represents a critical area to analyze for potential failure risks.

To calculate the theoretical minimum number of pinion teeth required to mesh with the 75-tooth gear D,

$$N_P = \frac{2k}{(1+2m)\sin^2\phi}(m + \sqrt{m^2 + (1+2m)\sin^2\phi})$$

where k is the tooth depth coefficient, m is the gear ratio, and ϕ represents the pressure angle.

Assuming standard parameters ($k = 1, \phi = 20^\circ$), the calculation indicates that the minimum number of teeth required to avoid interference is approximately 17 teeth. Since $N_{Actual}(9) < N_{min}(17)$, this confirms the interference. If manufactured as a standard gear, the roots of the teeth would be significantly undercut, which would reduce the bending strength of the gear.

However, potential mitigation strategies that the manufacturer might have employed could be to utilize stub teeth ($k = 0.8$) instead of full depth teeth, which are less likely to interfere. Limitations such as increasing the pressure angle from 20° to 25° could decrease the minimum tooth count requirement, potentially making the 9-tooth design a viable option.

1.4 Force Analysis

The component selected for stress analysis is pinion C, which is part of the second stage of the gear train reduction process. As the smallest gear in the high-torque stage, it is expected to experience the highest stress per tooth. Since standard gear failure most often occurs through bending fatigue at the root of the tooth, verifying the force and stress applied to this pinion is critical for determining the appropriate material and predicting the component's factor of safety.

To determine the torque load on gear C, the speed of gear C was calculated at this specific gear stage,

$$N_C = \frac{N_{motor}}{R_{belt}} = \frac{13,549.5}{94/13} \approx \mathbf{1,874} \text{ RPM}$$

Using the power formula ($P = T \cdot \omega$) with 300W power (assuming 100% transmission),

$$T_C = \frac{300 \text{ W}}{1,874 \text{ RPM} \times \frac{2\pi}{60}} \approx \mathbf{1.53} \text{ Nm}$$

With the pitch diameter ($d \approx 14 \text{ mm} = 0.014 \text{ m}$), the tangential contact force is

$$W_t = \frac{2 \times T_C}{d} = \frac{2 \times 1.53}{0.014} \approx \mathbf{218.57} \text{ N}$$

Assuming the standard 20° pressure angle (ϕ), the radial contact force is the separating force pushing the gears apart:

$$W_r = W_t \cdot \tan(20^\circ) = 218.57 \cdot 0.364 \approx \mathbf{79.55}\ \text{N}$$

The Lewis Equation was utilized to determine if the tooth of the gear will fail when the tooth is bending as it spins. In this equation, the Lewis Form Factor (Y) was assumed to be approximately 0.20. Because the gear has a significantly smaller number of teeth and was not included in the standard table, this value was estimated using the lowest tabulated entry, corresponding to 10 teeth $(Y \approx 0.201)$. The value for the module (m) was also derived from this equation ($m = \frac{d}{N}$).

$$\sigma = \frac{W_t}{F \cdot m \cdot Y}$$

$$\sigma = \frac{218.57}{12 \cdot 1.56 \cdot 0.20} \approx \mathbf{50.76}\ \text{MPa}$$

1.5 Material Selection

Based on the calculated stress of 50.76 MPa, there are three common gear materials that could be selected for pinion C. The following table identifies the key characteristics of the three materials:

Material	Yield Strength	Pros	Cons
Acetal	65 MPa	Low friction and quiet	Higher risk of failure
Glass Filled Nylon (30%)	148 MPa	Strong and lightweight	Wears down quickly
Sintered Steel	400+ MPa	Very durable and cheap	Heavier and louder

Figure 2: Table of Common Gear Materials.

To evaluate which material provides the highest reliability, a factor of safety (FoS) analysis was performed to assess the overall safety of the design. For gear applications, a commonly accepted guideline is to target a factor of safety greater than 2.0 in order to accommodate unexpected loads.

For acetal, the FoS value was calculated to be roughly 1.27, which is extremely close to failure and extensive loads could snap the teeth.

$$FoS = \frac{65\ \text{MPa}}{50.76\ \text{MPa}} \approx \mathbf{1.27}$$

For 30% glass-filled nylon, the FoS value was 2.94, leaving a comfortable safety margin for a household appliance.

$$FoS = \frac{148\ \text{MPa}}{50.76\ \text{MPa}} \approx \mathbf{2.92}$$

For sintered steel, the FoS value was approximately 7.88, indicating that the teeth will essentially never break under normal loads.

$$FoS = \frac{400\ \text{MPa}}{50.76\ \text{MPa}} \approx \mathbf{7.88}$$

Out of the three options, the ideal choice would be to pick the 30% glass-filled nylon, as it offers a high factor of safety, while keeping the gear fairly lightweight and quieter than metal. Choosing sintered steel would also be a viable option as with a factor of safety greater than 7, the material will have greater durability. However, using a steel pinion when gear D is made with standard plastic material will degrade the softer plastic gear over time. It would be best to avoid acetal for this specific 9-tooth pinion, as the stress of 50.76 MPa does not leave a huge margin to the limit.

1.6 Failure Modes

Based on the analyses above, two primary failure modes must be considered. Of these, bending fatigue is the most critical. Each time a gear tooth engages, the transmitted load induces bending stresses in the material. Over-extended use, these repeated stress cycles can initiate small cracks at the tooth root, eventually leading to tooth fracture. Additionally, because the 9-tooth pinion experiences interference, the manufacturing process would require material removal near the root. This reduction in tooth thickness increases stress concentrations, thereby accelerating fatigue damage and shortening the tooth's fatigue life.

Even if the gear tooth is sufficiently strong to resist structural failure, surface failure may still occur. As previously discussed, pairing a steel pinion with a plastic gear can lead to progressive wear of the softer plastic material, particularly if lubrication degrades or becomes contaminated.

MOTOR TRANSMISSION AND BELT DRIVE

The motor transmission system is designed to transfer power from a 120V, 300W brushless DC (BLDC) motor to the downstream reduction stages.



Figure 3: Motor.

The belt provides reliable, low-slip motor transmission.The use of a toothed belt minimizes slip and allows for consistent angular velocity under a load. The belt system combined with the gear reduction system described in the previous section transmits motion from the motor to the planetary gearbox. The planetary gear system delivers a controlled mixing motions, enabling interchangeable attachments such as the whisk, beater, and dough hook.



Figure 4: Belt and Motor System.

The toothed belt drive is identified as a PowerGrip GT (PDDT) type made out of polyamide. Its teeth shape is shown in the figure below [2].

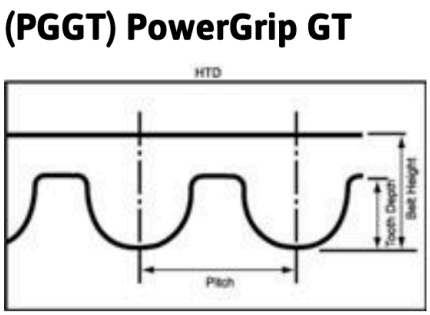


Figure 5: PowerGrip GT Teeth Shape.

2.1 Belt Tension Analysis

The rpm of the motor can be calculated by multiplying the rpm of the kitchen aid value by the gear reduction ratio.

$$N_a = 225\,rpm \times 60.22$$
$$N_a = 13,556\ rpm$$

In belt-driver systems, elastic stretching of the belt can lead to differences in theoretical and actual belt speeds, specifically as belt tensions and pulley diameters increase. Belt tension and

pulley geometry influence the speed and torque transmission of the system.

The belt pitch diameter can be calculated with the number of teeth as well as belt pitch.

$$D = \frac{Np}{\pi} = \frac{128(2mm)}{\pi}$$

$$D = 81.487\,mm$$

The belt linear speed can be calculated with the angular speed of the pinion as well as the belt pitch diameter.

$$v = \omega_a D\frac{\pi}{2} = 1,419\,\frac{rad}{s} \cdot 0.081487\,m \cdot \frac{\pi}{2}$$

$$v = 181.63\,m/s$$

The torque of gear b is needed to calculate the tension of driven gear. The angular speed is calculated using ratios with the number of teeth and the angular speed of gear a. That can be inserted into the torque equation using power.

$$\omega_b = \omega_a \frac{N_a}{N_b} = 1419\,rad/s \cdot \frac{13}{94}$$

$$\omega_b = 196.38\,rad/s$$

$$\tau_b = \frac{P}{\omega_b} = \frac{300W}{196.38\,rad/s}$$

$$\tau_b = 1.53\,N$$

The equation below connects the torque applied at the pulley to the difference between the tight side and slack side belt tensions.

$$\Delta F = F_1 - F_2 = \frac{2\tau}{D}$$

Tension around driving gear:

$$T_1 = \Delta F_b = \frac{2(0.21\,N)}{0.0112m} = 18.84\,N$$

Tension around driven gear:

$$T_2 = \Delta F_a = \frac{2(1.53\,N)}{0.087\,m} = 35.17\,N$$

The driven pulley exhibits a larger tension difference due to its higher torque at lower angular speed, while the driving pulley requires a smaller tension difference to transmit the same power.

2.3 Slip No-Slip Conditions

The belt drive is designed to operate under a no-slip condition due to the toothed belt which provides more friction between the belt and gear teeth. Unlike flat belts, timing belts reduce the likelihood of belt slip during operations and allows the angular and linear speed to be controlled by the teeth counts.

An analytical slip assessment was attempted using standard equations to relate the ratio of the tight and slack side belt tensions to the coefficient of friction and angle of wrap. However, this method is applied to flat friction-driven belts to verify no slip conditions. Available reference tables from the textbook apply primarily to flat and V-belt systems and do not accurately apply to toothed belt behavior.

Despite low likelihood of slip due to the teeth characteristics on the belt, ineffective motor transmission could still occur under certain conditions. Potential mechanisms include teeth wear, torque spikes during startup of the mixer or sudden loading, or pulley misalignment.

BEARINGS

The mixer uses three sealed deep groove ball bearings. Two identical bearings are stacked vertically on the shaft between gears B and C. A larger bearing of the same type is located on the motor where the shaft connects to gear A. This bearing is the most critical as it is closed to the applied loads of the gear train and sees the

largest combined radial loading. Focusing the analysis on the most heavily loaded bearing provides a conservative, worst-case design check. The purpose of the calculations detailed below is to verify the bearing safety and life compared to the design performance ratings relative to the manufacturer's dynamic load ratings of 3.45 kN provided by SKF [3].





Figures 6 and 7: Bearing in Mixer, Bearing.

3.1 Desired Life & Rotations

It is estimated that an amateur baker uses a mixer about one hour a week with a desired life of five years. The desired hours of use before failure is calculated below.

$$\mathcal{L}_D = \frac{1\ hr}{1\ wk} \cdot \frac{52\ wks}{1\ yr} \cdot 5\ yrs$$

$$\mathcal{L}_D = 260\ hrs$$

The number of revolutions through the 5 years of use can be calculated using the rotations per minute calculated in section two .

$$\#\,rev = 260\ hrs \cdot \frac{60\ mins}{1\ hr} \cdot \frac{13{,}556\ rot}{1\ min}$$

$$\#\,rev = 212 \times 10^6\ rotations\ over\ 5\ yrs$$

3.2 Bearing Loads

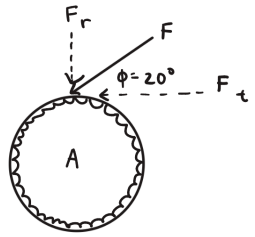
The bearing experiences radial loading only originating from the gear mesh forces at the driving gear A and the belt tension forces from the pulley system. Axial loads are neglected as spur gears do not generate axial loads; the belt drive is assumed to act purely radially on the shaft.

The tangential force exhibited by gear A is computed using the transmitted torque and pitch diameter.

$$F_T = \frac{\tau_a}{D_a} = \frac{2 \cdot 0.211\ N{\cdot}m}{0.0112\ m}$$

$$F_T = 37.68\ N$$

The radial force component is calculated from the gear pressure angle of $\phi = 20°$ which is standard for spur gears.



$$F_r = F_t tan(\phi) = 37.68\ tan(20)$$

$$F_r = 13.71\ N$$

These components were combined to obtain the magnitude of the resultant gear force acting radially on the bearing. While the bearing does not carry the entire gear force directly, this resultant provides a conservative estimate of the load transmitted through the shaft to the support.

$$F_{gear} = \sqrt{F_t^2 + F_r^2}$$

$$F_{gear} = \sqrt{37.68^2 + 13.71^2}$$

$$F_{gear} = 40.1\ N$$

The belt load acting on the shaft was calculated using the total of the tight and slack side tensions. This represents the net radial load applied by the belt to the pulley and transmitted onto the shaft. This method assumes that the belt force acts perpendicularly to the shaft axis.

$$F_{belt} = T_1 + T_2 = 18.84\,N + 35.17\,N$$

$$F_{belt} = 54.01\,N$$

The gear and belt forces were then added together to obtain the total radial load on the bearing. This method neglects the approximately 5 mm shaft distance between the applied loads and the bearing, which in reality would reduce the bearing reaction. Ignoring this creates a conservative analysis as it intentionally overestimates the bearing loads.

$$F_{R,\,total} = F_{gear} + F_{belt} = 40.1\,N + 54.01\,N$$

$$F_{R,\,total} = 94.11\,N$$

3.3 Bearing Type & Equivalent Loads

The bearing was measured to have an outer diameter of 30.1 mm and is a deep groove ball bearing. Therefore, table 11-2 was used to gather values of $C_0 = 2.24\,kN$ and $C_{10} = 5.07\,kN$.

Table 11–2

Dimensions and Load Ratings for Single-Row 02-Series Deep-Groove and Angular-Contact Ball Bearings

Bore, mm	OD, mm	Width, mm	Fillet Radius, mm	Shoulder Diameter, mm d_s	Shoulder Diameter, mm d_H	Load Ratings, kN Deep Groove C_{10}	Load Ratings, kN Deep Groove C_0	Load Ratings, kN Angular Contac C_{10}	Load Ratings, kN Angular Contac C_0
10	30	9	0.6	12.5	27	5.07	2.24	4.94	2.12
12	32	10	0.6	14.5	28	6.89	3.10	7.02	3.05
15	35	11	0.6	17.5	31	7.80	3.55	8.06	3.65
17	40	12	0.6	19.5	34	9.56	4.50	9.95	4.75
20	47	14	1.0	25	41	12.7	6.20	13.3	6.55
25	52	15	1.0	30	47	14.0	6.95	14.8	7.65
30	62	16	1.0	35	55	19.5	10.0	20.3	11.0
35	72	17	1.0	41	65	25.5	13.7	27.0	15.0
40	80	18	1.0	46	72	30.7	16.6	31.9	18.6
45	85	19	1.0	52	77	33.2	18.6	35.8	21.2
50	90	20	1.0	56	82	35.1	19.6	37.7	22.8
55	100	21	1.5	63	90	43.6	25.0	46.2	28.5
60	110	22	1.5	70	99	47.5	28.0	55.9	35.5
65	120	23	1.5	74	109	55.9	34.0	63.7	41.5
70	125	24	1.5	79	114	61.8	37.5	68.9	45.5
75	130	25	1.5	86	119	66.3	40.5	71.5	49.0
80	140	26	2.0	93	127	70.2	45.0	80.6	55.0
85	150	28	2.0	99	136	83.2	53.0	90.4	63.0
90	160	30	2.0	104	146	95.6	62.0	106	73.5
95	170	32	2.0	110	156	108	69.5	121	85.0

Figure 8: Table 11-2 Load Ratings [4].

Based on the estimation that the total axial load is zero, the axial load ratio is therefore zero, and $\frac{F_a}{v\,F_r} \leq e$. This indicates that the bearing is under the regime where radial load dominates.

Using table 11-1, it can be estimated that $x_1 = 1$ and $y_1 = 0$

F_a/C_0	e	$F_a/(VF_r) \leq e$ X_1	$F_a/(VF_r) \leq e$ Y_1	$F_a/(VF_r) > e$ X_2	$F_a/(VF_r) > e$ Y_2
0.014*	0.19	1.00	0	0.56	2.30
0.021	0.21	1.00	0	0.56	2.15
0.028	0.22	1.00	0	0.56	1.99
0.042	0.24	1.00	0	0.56	1.85
0.056	0.26	1.00	0	0.56	1.71
0.070	0.27	1.00	0	0.56	1.63
0.084	0.28	1.00	0	0.56	1.55
0.110	0.30	1.00	0	0.56	1.45
0.17	0.34	1.00	0	0.56	1.31
0.28	0.38	1.00	0	0.56	1.15
0.42	0.42	1.00	0	0.56	1.04
0.56	0.44	1.00	0	0.56	1.00

*Use 0.014 if $F_a/C_0 < 0.014$.

Figure 9: Table 11.1 Equivalent Radial Load Factors for Ball Bearings [4].

3.4 Dynamic Load Bearing

The equivalent dynamic bearing load was used in the ABMA C_{10} life equation to determine the required dynamic load rating, which corresponds to the desired operating life at 90% reliability.

$$C_{10} = F_D\left(\frac{L_D}{L_R}\right)^{1/a} = F_D\left(\frac{\mathcal{L}_D n_D 60}{\mathcal{L}_R n_R 60}\right)^{1/a}$$

$$F_D = F_r \rightarrow axial\ load = 0$$

$$\mathcal{L}_D = 260\,hrs$$

$$n_D = 13,556\,rpm$$

$$\mathcal{L}_R = 10^6 \rightarrow ABMA$$

$$a = 3 \rightarrow ball\ bearing$$

$$C_{10} = 94.11\,N\left(\frac{260\,hr \cdot 13556 rpm \cdot 60}{10^6}\right)^{1/3}$$

$$C_{10} = 286\,N = 0.286\,kN$$

The C_{10} value calculated is compared to the manufacturer's dynamic load rating of 3.45 kN for the motor bearing. Because the catalog rating is larger than the required value, the bearing

satisfies the ABMA life and safety criteria under the assumed loading conditions.

$$3.45\,kN \;\geq\; 0.28\,kN$$

TILT LOCK SHAFT AND SPRING SYSTEM

The tilt lock system is responsible for securing the top half of the mixer into either the downwards in-use position or the upwards tilted position. This mechanism, controlled by a button above the mixing speed control dial, allows the user to easily access the contents of the mixing bowl while it is on the base of the stand.



Figure 10: Tilt Lock Button on Kitchen in the Box Mixer.

When tearing down the Kitchen in a Box stand mixer, the locking mechanism remained intact and functional with all parts removed. In fact, the mechanism proved to be surprisingly sturdy, as the rod of the locking button withstood the force of two group members trying to break the shell of the mixer into its two halves.

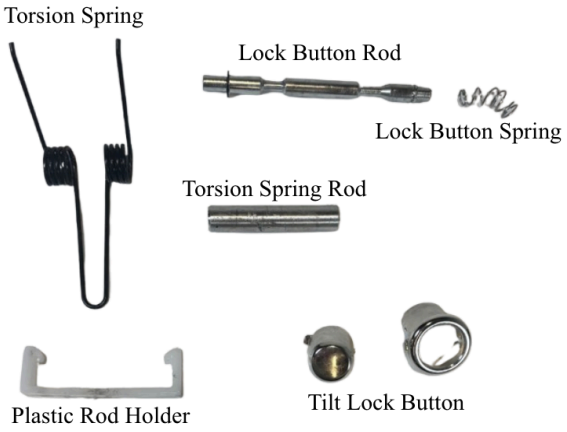


Figure 11: Components of the Tilt Lock Shaft and Spring System.

The placement of the locking button rod within the plastic shell made the hardware difficult to access and remove. The limitation of rotation from the rod also prevented the evaluation of the pivot point. Once a small, C-shaped metal piece was removed from the rod, it fell through the hole in the shell where the tilt lock button once was. This made it possible to separate the two halves of the mixer, revealing the torsion spring system at the pivot point.

4.1 Torsion Spring Analysis

The torsion spring system allows for the ease of use of the tilt lock mechanism by creating torsion to help lift the top half of the mixer to the tilted position and provide resistance when bringing the top half down to the in-use position. The torsion spring rate

$$k = \frac{\text{Applied Torque}}{\text{Angle of Deflection}}$$

was found experimentally using a digital force gauge, calipers, and a protractor to measure the applied torque and angle of deflection.



Figure 12: Force Gauge Reading 13 N.

The torsion spring has a resting angle of 125°. The force gauge was attached to the top of the torsion spring with a carabiner, and the force was applied approximately perpendicular to the moment arm, so that the applied torque

$$\vec{T} = \vec{r} \times \vec{F} \implies T = rF$$

simplifying calculations and measurements. The force was also applied until the spring's arms made a 90° angle, as pictured above. The force gauge reads 13 N, the spring's arm is 7.2 cm, and the angle of deflection from the resting 125° is 35°, therefore

$$k = \frac{rF}{\Delta\theta} = \frac{(0.072\ \text{m})(13\ \text{N})}{(35^\circ)(\frac{\pi}{180})} = 1.53\ \frac{\text{N}\cdot\text{m}}{\text{rad}}$$

With the torsion spring rate, the applied torque and stress can be calculated.

$$k = \frac{T}{\Delta\theta} \implies T = k\Delta\theta$$

When the mixer is in the ready position, the torsion spring's arms are parallel; therefore, the angle of deflection is 125°, or 2.18 radians.

$$T = (1.53\ \frac{\text{N}\cdot\text{m}}{\text{rad}})(2.18\ \text{rad}) = 3.34\ \text{N}\cdot\text{m}$$

When the mixer is in the tilted position, the torsion spring's arms are 30.6° above parallel; therefore the angle of deflection is 94.4° or 1.65 radians.

$$T = (1.53\ \frac{\text{N}\cdot\text{m}}{\text{rad}})(1.65\ \text{rad}) = 2.52\ \text{N}\cdot\text{m}$$

With the applied torques known, the stress in the wire can be calculated.

$$\sigma = K_B \frac{32T}{\pi d^3}$$

where

$$K_B = \frac{4C^2 - C - 1}{4C(C-1)}$$

is the correction factor to account for additional stress concentrations [4]. The spring index C (7.19) is the ratio of the mean coil diameter (15.1 mm) to the wire diameter (2.1 mm).

$$K_B = \frac{4(7.19)^2 - 7.19 - 1}{4(7.19)(7.19-1)} = 1.12$$

Now calculating stress,

$$\sigma_{\text{in use}} = \frac{(1.12)(32)(3.34)}{(\pi)(2.1\times10^{-3})^3} = 4110\ \text{MPa}$$

$$\sigma_{\text{tilted}} = \frac{(1.12)(32)(2.52)}{(\pi)(2.1\times10^{-3})^3} = 3100\ \text{MPa}$$

These stresses are very high, so there were most likely inaccuracies when determining the spring rate from the force gauge. Considering that the spring is a double torsion spring (two coils instead of one) makes the stresses more reasonable (half of the stress per coil) which puts the wire at the upper end of the range strength for hard-drawn wire.

4.2 Tilt Lock Button System

The tilt lock button system contains a spring and a rod. The spring provides the functionality of the button itself, while the rod secures the upper half of the mixer into the in-use or tilted position. Since the spring and shaft play such different roles in the tilt lock button system, these components can be analyzed separately.

4.2.1 Tilt Lock Button Spring Analysis

The spring constant of the button was found experimentally by hanging a known weight from the end of the spring and measuring its deflection. The spring measured 2.1 cm unstretched and 3.1 cm stretched with a 3 lb weight on one end. Since the forces must be equal and opposite,

$$mg = kx \implies k = \frac{mg}{x}$$
$$k = \frac{(1.36\text{ kg})(9.81\frac{\text{m}}{\text{s}^2})}{(0.01\text{ m})} = 133.4\ \frac{\text{N}}{\text{m}}$$

The force required for the user to push the button can be calculated using the spring constant and the height difference of the button when unpressed versus pressed, 1.1 cm.

$$F = kx = (133.4\ \frac{\text{N}}{\text{m}})(0.011\text{ m}) = 1.47\text{ N}$$

The tilt lock button requires 1.47 N of force to press. The button only requires a light press, so this number seems somewhat reasonable. A more ideal experiment would determine the deflection from compression.

The spring's torsional shear stress

$$\tau = K_B\frac{8Fd}{\pi d^3}$$

with Bergstrasser correction factor

$$K_B = \frac{4C+2}{4C-3}$$

can be determined knowing the applied force and characteristics of the spring [4].

$$C = \frac{D}{d} = \frac{7.8\text{mm}}{0.8\text{mm}} = 9.75$$
$$K_B = \frac{4(9.75)+2}{4(9.75)-3} = 1.14$$
$$\tau = (1.14)\frac{8(1.47)(7.8\times10^{-3})}{\pi(0.8\times10^{-3})}$$
$$\tau = 65.0\text{ MPa}$$

This is well below the yield strength of hard drawn steel springs which aligns with expectations because there is only a small force being applied to the button and spring.

4.2.2 Tilt Lock Rod Analysis

When the tilt lock button is pressed, a metal rod is pushed in to align the narrower cross-section of the rod to the path on the shell which allows the user to tilt the mixer. When the button is not pressed, the rod and the shell of the bottom half of the mixer bear the weight of the upper half in either the tilted or ready-to-use position. By creating a 3D model and performing a study in SolidWorks, the failure point and factor of safety of the rod can be determined.

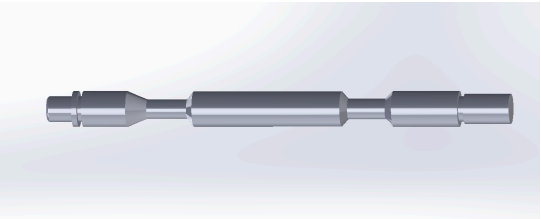


Figure 13: Tilt Lock Rod CAD Model.

AISI 1020 steel was selected as the material. Because the rod is intended to have high strength and does not have to be ductile, cold rolled was also selected. At first glance, it appears that the rod would fail at the least thick sections, however this is not where the force is applied. Load is not applied in these areas because they are simply to allow for movement.

After closely observing the button movement, the two points of contact were determined to be on the center and right sections. Finite element analysis was performed, applying forces of increasing magnitudes at the determined points until the bar failed.

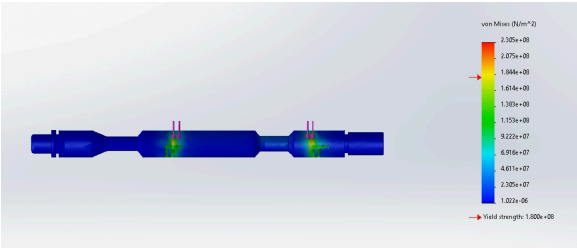


Figure 14: Tilt Lock Rod Finite Element Analysis.

The bar failed under 2000 N of force, 1000 N applied at each point. The red arrow indicates the yield strength of the material, and the scale shows the von Mises stress. The bar will yield at the yellow areas, where the force is applied.

In order to determine the factor of safety, the load applied must be estimated. The Kitchen in the box mixer weighs seven pounds which translates to roughly 30 Newtons of force. For a conservative estimate, the entire weight of the mixer can be used to determine the factor of safety, rather than trying to estimate the weight of the top half of the mixer. The bar also must withstand the force of the upper half of the mixer suddenly dropping onto it if the user puts the mixer in the ready-to-use position from the tilted position without caution, approximately 50 N. Finally, the user may apply additional force to the rod to ensure the mixer is locked into the correct position, approximately 50 N. (Both of these scenarios occurred during the testing of this product.) This estimates a conservative total of 130 N force applied to the mixer during regular use.

$$FoS = \frac{2000\ \text{N}}{130\ \text{N}} = 15.4$$

The rod has a very high factor safety which was evident when the bar withstood high forces during the group's initial attempts to separate the two halves of the mixer during the product teardown. The bar is very unlikely to be the cause of the lock button system breaking.

CONCLUSION

The Kitchen in the Box Stand Mixer demonstrates thoughtful engineering that balances performance and cost, though analysis reveals several vulnerabilities that may limit long-term reliability. While the bearings and tilt lock system are substantially over-designed with high safety margins, the gear train presents the most significant concern for product longevity.

The 9-tooth pinion C represents the primary failure point in the system. Operating below the 17-tooth interference threshold creates stress concentrations of 50.76 MPa at the tooth root which approaches the material limit, even with 30% glass-filled nylon. Under repeated cyclic loading, this component is highly susceptible to bending fatigue, particularly as material removal during manufacturing further weakens the tooth structure. Users who exceed the assumed one-hour-per-week usage pattern or frequently process high-viscosity materials like bread dough will accelerate fatigue crack initiation at this location.

Secondary concerns include surface wear of the plastic gears, especially if paired with harder materials or if the lubrication degrades over time. The belt drive system is designed to prevent slip through its toothed belt, but is vulnerable to tooth wear and potential failure during startup torque spikes or pulley misalignment. Additional factors affecting longevity include grease degradation leading to increased friction and wear throughout the gear system, and damage from user error such as water or impact from dropping.

Overall, the mixer is appropriately designed for its intended consumer application of moderate home use. Minimal tooth counts and plastic gearings enable a compact, cost-effective design, but create vulnerabilities that could result in premature failure. The product should reliably serve amateur bakers within its design parameters, but heavy users should anticipate potential gear train failure as the most likely end-of-life mechanism.

REFERENCES

[1] KitchenAid Commercial 8-Quart Stand Mixer with Bowl Guard, EverythingKitchens. [Online]. Available:https://www.everythingkitchens.com/kitchenaid-commercial-8-quart-stand-mixer-with-bowl-guard-white-ksmc895wh.html

[2] PowerGrip™ GT™3 Rubber Synchronous Belts, Gates Corporation. [Online]. Available: https://www.gates.com/us/en/power-transmission/synchronous-belts/rubber-synchronous-belts.p.9356-000000-000000.html

[3] *SKF 608-Z Deep Groove Ball Bearing*, SKF. [Online]. Available: https://www.skf.com/us/products/rolling-bearings/ball-bearings/deep-groove-ball-bearings/productid-608-Z

[4] R. G. Budynas and J. K. Nisbett, Shigley's Mechanical Engineering Design, 10th ed., New York, NY, USA: McGraw-Hill Education, 2014. ISBN: 978-0-07-339820-4.